

# Stability Analysis and Control Design for an Underactuated Walking Robot via Computation of a Transverse Linearization<sup>\*</sup>

Leonid B. Freidovich<sup>\*</sup> Anton S. Shiriaev<sup>\*,\*\*</sup> Ian R. Manchester<sup>\*</sup>

<sup>\*</sup> Department of Applied Physics and Electronics,  
Umeå University, SE-901 87 Umeå, Sweden

{leonid.freidovich,anton.shiriaev,ian.manchester}@tfe.umu.se

<sup>\*\*</sup> Department of Engineering Cybernetics, Norwegian University of  
Science and Technology, NO-7491 Trondheim, Norway

**Abstract:** The problem is to create a hybrid periodic motion, reminiscent of walking, for a model of an underactuated biped robot. We show how to construct a transverse linearization analytically and how to use it for stability analysis and for design of an exponentially orbitally stabilizing controller. In doing so, we extend a technique recently developed for continuous-time controlled mechanical systems with degree of underactuation one. All derivations are shown on an example of a three-link walking robot, modeled as a system with impulse effects.

Keywords: Walking robots; Systems with impulse effects; Transverse linearization; Orbital stability; Nonlinear feedback control

## 1. INTRODUCTION

Planning and stabilizing periodic motions in underactuated mechanical systems is a challenging task. One of the powerful tools for feedback control design and closed-loop system stability analysis is computation of a transverse linearization in a vicinity of the desired orbit.

Roughly speaking, an  $n$ -dimensional nonlinear system in the vicinity of a periodic orbit can be decomposed, by an appropriate change of coordinates, into two coupled subsystems: (a) a scalar system representing the dynamics along the cycle, and (b) an  $(n-1)$ -dimensional system representing dynamics transverse to the cycle. The *transverse linearization* is the linearization of this second subsystem about the desired orbit, and is an  $(n-1)$ -dimensional linear system with periodic coefficients. An overview of some recent advances using this approach for mechanical systems without impacts can be found in [12].

The main goal of this paper is to show how to extend this analytical technique for the class of underactuated mechanical systems with underactuation degree one with impulse effects, modeling impacts with the environment.

We should notice that the concept of transverse linearization has been used in a similar content in [15], where a numerical procedure, based on the notion of orthogonalizing transform, has been proposed. What distinguishes our approach is that we provide an explicit *analytical* construction for such a linearization for a known cycle.

We take an example from a seminal work [6], where a new design strategy for creating stable hybrid periodic

motions for a class of models suggested for planar biped robots has been proposed. We simplify the controller to make it more suitable for implementation by removing not differentiable nonlinearities. The new closed-loop system lacks the property of finite-time convergence to a certain manifold and therefore can not be analyzed using the technique presented in [6, 19, 18]. We analytically compute a transverse linearization and prove orbital exponential stability.

Remarkably, it is straightforward to investigate robustness with respect to uncertainty in physical parameters exploiting our computed linear comparison system; although, we will not deviate in this direction. Finally, we suggest another family of stabilizing controllers.

### 1.1 A Model for a Three-Link Biped

Following [5, 6], the Lagrangian dynamics [17] of a simple three-link planar biped during the swing phase of motion can be described by the following equations

$$\begin{aligned} & \frac{5}{2} \left( \frac{25}{2} \ddot{q}_1 - \cos(q_1 - q_2) \ddot{q}_2 + 2 \cos(q_3 - q_1) \ddot{q}_3 \right. \\ & \quad \left. - 2 \sin(q_3 - q_1) \dot{q}_3^2 - \sin(q_1 - q_2) \dot{q}_2^2 - 13g \sin q_1 \right) = -u_1, \\ & \frac{5}{2} \left( \frac{1}{2} \ddot{q}_2 - \cos(q_1 - q_2) \ddot{q}_1 + \sin(q_1 - q_2) \dot{q}_1^2 + g \sin q_2 \right) = -u_2, \\ & 5 \left( \cos(q_3 - q_1) \ddot{q}_1 + \frac{1}{2} \ddot{q}_3 + \sin(q_3 - q_1) \dot{q}_1^2 - g \sin q_3 \right) = u_1 + u_2, \end{aligned} \quad (1)$$

where the numerical values of the parameters are taken from [5, 6];  $g = 9.8$  is the acceleration due to gravity;  $q_1, q_2, q_3$  are some generalized coordinates in the inertia frame defining the positions of the stance leg, the swing leg, and the torso, respectively;  $u_1, u_2$  are the controlled torques applied between the legs and the torso.

<sup>\*</sup> This work has been partly supported by the Swedish Research Council (grants: 2005-4182, 2006-5243) and the Kempe Foundation.

This model can be rewritten compactly as:

$$M(q)\ddot{q} + C(q, \dot{q})\dot{q} + G(q) = Bu \quad \text{and} \quad \dot{x}(t) = f(x(t), u)$$

using the standard notation [17] for the inertia matrix  $M(q)$ , the matrix of Coriolis and centrifugal forces  $C(q, \dot{q})$ , the vector of generalized gravitational forces  $G(q)$ , and with  $q = [q_1, q_2, q_3]^T$ ,  $\dot{q} = [\dot{q}_1, \dot{q}_2, \dot{q}_3]^T$ ,  $u = [u_1, u_2]^T$ , and  $x = [q_1, q_2, q_3, \dot{q}_1, \dot{q}_2, \dot{q}_3]^T$ .

Some simplifying hypothesis are assumed deriving such a model. In particular, the results reported in [9], allow us, to a certain extent, ignoring the possibility of interaction of the swing leg with the ground during the swinging phase.

The continuous-time dynamics above is valid only before an impact with the ground occurs at the moment when  $q_1$  (the stance leg) reaches the value of  $\pi/8$ , i.e. when the solution of (1) hits the smooth surface

$$\Gamma_- = \{x = [q_1, q_2, q_3, \dot{q}_1, \dot{q}_2, \dot{q}_3]^T \in \mathbb{R}^6 : q_1 = \pi/8\}. \quad (2)$$

The impact is modeled, under some simplifying hypothesis (see [8]), by the instantaneous map  $F(\cdot)$  defined by [5]:

$$q_i(t_+) = q_i(t_-) \quad \text{and} \quad \dot{q}_i(t_+) = \omega_i(q(t_-), \dot{q}(t_-)), \quad (3)$$

where  $i \in \{1, 2, 3\}$ , and the arguments  $t_-$  and  $t_+$  denote the values right before and right after the impact, respectively, and

$$\omega_1(q, \dot{q}) = 5 \left( \dot{q}_1 - 20\dot{q}_1 \cos(2q_1 - 2q_2) + 4\dot{q}_1 \cos(2q_3 - 2q_1) + 2\dot{q}_2 \cos(2q_1 - 2q_2) \right) / \Delta(q),$$

$$\omega_2(q, \dot{q}) = 10 \left( 2\dot{q}_1 \cos(2q_3 - q_1 - q_2) - 9\dot{q}_1 \cos(q_1 - q_2) + \dot{q}_2 \right) / \Delta(q),$$

$$\omega_3(q, \dot{q}) = 5 \left( 12\dot{q}_1 \cos(q_1 + q_3 - 2q_2) - 12\dot{q}_1 \cos(q_1 - q_3) + \dot{q}_1 \cos(3q_1 - 2q_2 - q_3) - \dot{q}_2 \cos(q_2 - q_3) - \frac{19}{2}\dot{q}_3 + \dot{q}_3 \cos(2q_1 - 2q_2) + 2\dot{q}_3 \cos(2q_2 - 2q_3) \right) / \Delta(q)$$

$$\Delta(q) = -95 + 10 \cos(2q_1 - 2q_2) + 20 \cos(2q_2 - 2q_3). \quad (4)$$

After the impact, the stance leg and the swing leg are switched and the states evolve according to the continuous-time dynamics identical to (1) up to renaming.

The resulting hybrid dynamical system corresponds to the following evolution chart

$$\Gamma_+^{(1)} \xrightarrow{\dot{x}=\bar{f}_1(\cdot)} \Gamma_-^{(1)} \xrightarrow{F_1} \Gamma_+^{(2)} \xrightarrow{\dot{x}=\bar{f}_2(\cdot)} \Gamma_-^{(2)} \xrightarrow{F_2} \Gamma_+^{(1)}$$

and can be described as follows:

$$\left. \begin{aligned} x(t_{0+}) &\in \Gamma_+^{(1)}, \\ \dot{x}(t) &= \bar{f}_1(x(t), u) \quad \text{for } t_0 < t < t_1, \\ t_1 &\stackrel{def}{=} \arg \min \{t_1 > t_0 : x(t_{1-}) \notin \Gamma_-^{(1)}\}, \\ x(t_{1+}) &= F_1(x(t_{1-})) \in \Gamma_+^{(2)}, \\ \dot{x}(t) &= \bar{f}_2(x(t), u) \quad \text{for } t_1 < t < t_2, \\ t_2 &\stackrel{def}{=} \arg \min \{t_2 > t_1 : x(t_{2-}) \notin \Gamma_-^{(2)}\}, \\ x(t_{2+}) &= F_2(x(t_{2-})) \in \Gamma_+^{(1)}, \\ t_0 &\stackrel{def}{=} t_2 \quad (\text{redefine and restart}), \end{aligned} \right\} \quad (5)$$

where

$$\begin{aligned} \Gamma_-^{(1)} &= \Gamma_+^{(2)} = \Gamma_- = \{x \in \mathbb{R}^6 : q_1 = \pi/8\}, \\ \Gamma_+^{(1)} &= \Gamma_-^{(2)} = \Gamma_+ = F(\Gamma_-) = \{x \in \mathbb{R}^6 : q_2 = \pi/8\}, \\ \bar{f}_1(x(t), u) &= f(x(t), u), \quad F_1(x) = F(x), \\ \bar{f}_2(x(t), u) &= P^{-1} f(Px(t), u), \quad F_2(x) = F(Px), \end{aligned} \quad (6)$$

and the linear transformation  $P$  denotes renaming the legs ( $q_1 \leftrightarrow q_2$  and  $\dot{q}_1 \leftrightarrow \dot{q}_2$ ) and the symmetry of the legs is exploited to derive the expression for  $\bar{f}_2$  and  $F_2$ .

## 1.2 Motion Planning and Control Design from [6, 18]

Due to symmetry between the legs, in the case when a symmetric limit cycle (the one consisting of two identical steps) is of interest, it is possible to define the controllers for the first and the second parts of the continuous dynamics in a similar fashion. Following this way, we describe below the design for the first part only.

It has being shown in [6, 18] that:

(1) Defining the following outputs

$$\begin{aligned} y_{1c} &= q_2 - p_{y1c}(q_1) \equiv q_2 + q_1 - (a_5 + a_6 q_1 + a_7 q_1^2 + a_8 q_1^3), \\ y_{2c} &= q_3 - p_{y2c}(q_1) \equiv q_3 - (a_1 + a_2 q_1 + a_3 q_1^2 + a_4 q_1^3) \left( q_1^2 - \frac{\pi^2}{8} \right) \end{aligned} \quad (7)$$

with, see [5, 18],

$$\begin{aligned} a_1 &= 0.512, \quad a_2 = 0.073, \quad a_3 = 0.035, \quad a_4 = -0.819, \\ a_5 &= -2.27, \quad a_6 = 3.26, \quad a_7 = 3.11, \quad a_8 = 1.89, \end{aligned} \quad (8)$$

(2) Using the partial linearizing feedback transformation [16] with respect to these outputs

$$\begin{aligned} u &= \left( J_c(q_1, \dot{q}_1) \begin{bmatrix} 0_{3 \times 2} \\ M^{-1}(q)B \end{bmatrix} \right)^{-1} \begin{bmatrix} v_{1c} \\ v_{2c} \end{bmatrix} \\ &\quad - J_c(q_1, \dot{q}_1) \begin{bmatrix} \dot{q} \\ M^{-1}(q)(-C(q, \dot{q})\dot{q} - G(q)) \end{bmatrix}, \end{aligned} \quad (9)$$

$$\text{where } J_c(\theta, \dot{\theta}) = \begin{bmatrix} -p''_{y1c}(\theta)\dot{\theta}, 0, 0, -p'_{y1c}(\theta), 1, 0 \\ -p''_{y2c}(\theta)\dot{\theta}, 0, 0, -p'_{y2c}(\theta), 0, 1 \end{bmatrix}$$

so that (1) is equivalently rewritten in the form

$$\dot{y}_{1c} = v_{1c}, \quad \dot{y}_{2c} = v_{2c}, \quad \ddot{q}_1 = \dots,$$

where "... denote a lengthy expression, which is straightforward to compute.

(3) Applying the continuous finite-time stabilizing feedback [2]

$$\begin{aligned} v_{1c} &= -10^{\frac{11}{10}} \text{sign}(\dot{y}_{1c}) |\dot{y}_{1c}|^{\frac{9}{10}} - 10^2 \text{sign}(\phi_{1c}) |\phi_{1c}|^{\frac{9}{11}}, \\ \phi_{1c} &= y_{1c} + \frac{10^{\frac{9}{10}}}{110} \text{sign}(\dot{y}_{1c}) |\dot{y}_{1c}|^{\frac{11}{10}}, \\ v_{2c} &= -10^{\frac{11}{10}} \text{sign}(\dot{y}_{2c}) |\dot{y}_{2c}|^{\frac{9}{10}} - 10^2 \text{sign}(\phi_{2c}) |\phi_{2c}|^{\frac{9}{11}}, \\ \phi_{2c} &= y_{2c} + \frac{10^{\frac{9}{10}}}{110} \text{sign}(\dot{y}_{2c}) |\dot{y}_{2c}|^{\frac{11}{10}}, \end{aligned} \quad (10)$$

one achieves an exponentially orbitally stable periodic trajectory  $x_*(t)$  with two jumps in the closed-loop system. It has the half-period  $T_h \approx 1.12163$  sec. and corresponds to the jump due to impact with

$$\begin{aligned} x_*(T_h+) &= x_0 \approx [-0.392699, 0.392699, 0.496465, \\ &0.926751, -0.239267, 1.483783]^T \in \Gamma_+^{(1)}, \\ x_*(T_h-) &= x_T \approx [0.392699, -0.392699, 0.496466, \\ &1.549891, -2.031622, -0.431507]^T \in \Gamma_-^{(1)}. \end{aligned} \quad (11)$$

Asymptotic stability of the cycle has been shown in [6] using the fact that the controller (10) brings the trajectories to a two-dimensional manifold in a sufficiently short finite time. As a result, it is possible to obtain an appropriate restriction of the standard Poincaré first-return map, computation of which becomes traceable, for a rigorous proof of existence of an attractive limit cycle.

Later, the design procedure for the regulated outputs in the form (7) has been refined in [19] to make them invariant not only under the continuous part of the closed-loop dynamics (1), (9), (10) with (7) but also under the jump (3), (4) together with a subset of the intersection of the manifold with the surface (2). These outputs allow better interpretations and substitution of the controller (10) with a smooth one, providing sufficiently fast exponential convergence to the invariant manifold [10]. However, the described technique does not allow answering the following question: “*What happens if the part of the proposed feedback control law (10) with infinite slope is approximated by a smooth function, which is simpler for implementation?*” To be more precise, let us substitute the nonlinear functions in (10) by their least-squares linear approximations on some intervals:

$$\begin{aligned} v_{1c} &= -13.023 y_{1c} - 106.45 (y_{1c} + 0.0699 \dot{y}_{1c}) \\ v_{1c} &= -13.023 y_{2c} - 106.45 (y_{2c} + 0.0699 \dot{y}_{2c}) \end{aligned} \quad (12)$$

It turns out that the closed-loop system (5), (9), (12) has a periodic solution with two jumps which is close to the original one. It has the half-period  $T_h \approx 1.02418$  sec. and corresponds to the jump due to impact with

$$\begin{aligned} x_*(T_h+) &= x_0 \approx [-0.389494, 0.392699, 0.493776, \\ &0.945162, -0.233740, 1.480095]^T \in \Gamma_+^{(1)}, \\ x_*(T_h-) &= x_T \approx [0.392699, -0.389494, 0.493776, \\ &1.574679, -2.060533, -0.453536]^T \in \Gamma_-^{(1)}. \end{aligned} \quad (13)$$

Let us verify its stability.

### 1.3 Transverse Linearization for Continuous Dynamics

Since there exists a periodic hybrid trajectory  $q = q_*(t)$ :

$$q_1 = \theta_*(t), \quad q_2 = q_{2*}(t), \quad q_3 = q_{3*}(t) \quad (14)$$

in the closed-loop system, described in the previous section, there must exist two functions:  $\phi_1(\theta)$  and  $\phi_2(\theta)$ , defining an induced virtual holonomic constraint, such that each of the two outputs

$$y_1 = q_2 - \phi_1(q_1) \quad \text{and} \quad y_2 = q_3 - \phi_2(q_1) \quad (15)$$

is identically equal to zero along the target trajectory of the closed-loop hybrid system (5) with the control law defined above, so that:

$$q_{2*}(t) \equiv \phi_1(\theta_*(t)) \quad \text{and} \quad q_{3*}(t) \equiv \phi_2(\theta_*(t)). \quad (16)$$

Moreover, along the desired motion, the other variable  $q_1(t)$  coincides with the solution of the integrable projected dynamics in the form [13]

$$\alpha(\theta_*) \ddot{\theta}_* + \beta(\theta_*) \dot{\theta}_*^2 + \gamma(\theta_*) = 0, \quad (17)$$

initiated at  $\theta_*(0) = a$  and  $\dot{\theta}_*(0) = b$ , which are defined by the first and the fourth components<sup>1</sup> of  $x_0$  in (13).

In order to obtain the expressions for the functions in (17), it is sufficient to add the three differential equations in (1) and substitute  $q_2$  with  $\phi_1(\theta)$ ,  $q_3$  with  $\phi_2(\theta)$ , and  $q_1$  with  $\theta$ . The result is

$$\begin{aligned} \alpha(\theta) &= -\frac{5}{2}(1 + \phi_1'(\theta)) \cos(\theta - \phi_1(\theta)) \\ &+ 5(\phi_2'(\theta) + 1) \cos(\theta - \phi_2(\theta)) + \frac{5}{4}(25 + \phi_1'(\theta) + 2\phi_2'(\theta)), \end{aligned} \quad (18)$$

$$\begin{aligned} \beta(\theta) &= -\frac{5}{2}\phi_1''(\theta) \cos(\theta - \phi_1(\theta)) + 5\phi_2''(\theta) \cos(\theta - \phi_2(\theta)) \\ &+ 5\left((\phi_2'(\theta))^2 - 1\right) \sin(\theta - \phi_2(\theta)) \\ &+ \frac{5}{4}\phi_1''(\theta) + \frac{5}{2}\phi_2''(\theta) + \frac{5}{2}\left((1 - \phi_1'(\theta))^2\right) \sin(\theta - \phi_1(\theta)), \end{aligned} \quad (19)$$

$$\gamma(\theta) = \frac{5g}{2} \left( \sin(\phi_1(\theta)) - 2 \sin(\phi_2(\theta)) - 13 \sin(\theta) \right). \quad (20)$$

The phase portrait of the system (17) with (18), (19), and (20) for the closed-loop system with (10) is given in Fig. 1.

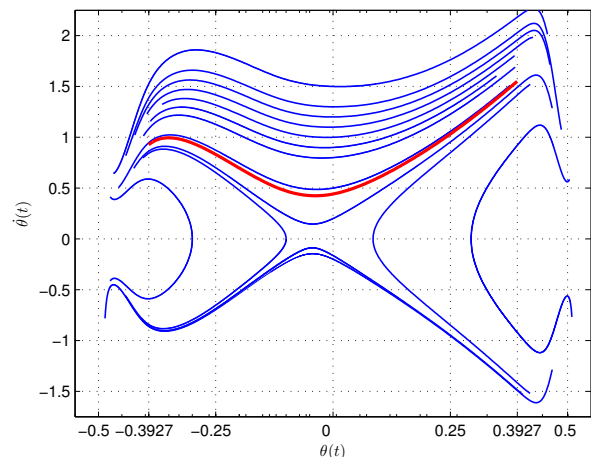


Fig. 1. A few solutions of the reduced dynamics (17), (18), (19), (20). The chosen motion  $\theta_*(t)$ , which is a part of an unbounded solution is shown in red.

It can be seen that the planned motion  $\theta_*(t)$  corresponds to a part of an unbounded solution around a saddle. This fact leads to degradation of the closed-loop system performance under small errors in approximations of the virtual constraints and in evaluation of the desired motion as well as under small parametric uncertainty. It is remarkable that despite this, the proposed controller has been experimentally successfully tested [4, 18].

Let us proceed with stability analysis and other issues.

The five coordinates describing the dynamics transverse to the desired orbit [12] are  $y_1$ ,  $y_2$ ,  $\dot{y}_1$ , and  $\dot{y}_2$ , defined by (15), and  $I(q_1, \dot{q}_1)$ , computed as [14]

<sup>1</sup> Note that the components of  $x_0$  and of  $x_T$  must be in agreement with  $y_1(0) = y_2(0) = 0$  and  $\dot{y}_1(0) = \dot{y}_2(0) = 0$  as well. Moreover,  $\theta_*(T_h-)$  and  $\theta_*(T_h+)$  are equal to the first and the fourth components of  $x_T$ , respectively.

$$I(\theta, \dot{\theta}) = \dot{\theta}^2 - \psi(\theta_*(0), \theta) \dot{\theta}_*(0)^2 + \int_{\theta_*(0)}^{\theta} \psi(s, \theta) \frac{2\gamma(s)}{\alpha(s)} ds,$$

$$\psi(s_1, s_2) = \exp \left\{ - \int_{s_1}^{s_2} \frac{2\beta(s)}{\alpha(s)} ds \right\} \quad (21)$$

from the functions (18), (19), and (20).

One way to derive a linearization of the transverse dynamics is as follows. One starts with rewriting the closed-loop system in terms of the new coordinates  $y_1, y_2, \theta = q_1$  and their derivatives. After straightforward but lengthy computations, one can obtain an equivalent description of the continuous part of the closed-loop system (1), (9), (10) with (7) in the form:

$$\ddot{y}_1 = v_1, \quad \ddot{y}_2 = v_2, \quad \ddot{\theta} = \dots + \dots \ddot{y}_1 + \dots \ddot{y}_2, \quad (22)$$

where “...” denote lengthy expressions, which are straightforward to compute, and

$$v_1 = f_1(\theta, \dot{\theta}, y_1, y_2, \dot{y}_1, \dot{y}_2) \quad \text{and} \quad v_2 = f_2(\theta, \dot{\theta}, y_1, y_2, \dot{y}_1, \dot{y}_2) \quad (23)$$

are the functions defined by

$$\begin{bmatrix} v_1 \\ v_2 \end{bmatrix} = J(\theta, \dot{\theta}) \begin{bmatrix} \dot{q} \\ M^{-1}(q)(Bu - C(q, \dot{q})\dot{q} - G(q)) \end{bmatrix}, \quad (24)$$

where  $u$  is given by (9), (10),

$$J(\theta, \dot{\theta}) = \begin{bmatrix} -\phi_1''(\theta)\dot{\theta}, 0, 0, -\phi_1'(\theta), 1, 0 \\ -\phi_2''(\theta)\dot{\theta}, 0, 0, -\phi_2'(\theta), 0, 1 \end{bmatrix}$$

and everything is expressed in the appropriate variables.

The next step is to substitute the first two equation of (22) into the last one. After that, the last equation can be rewritten in such a form that its left-hand side coincide with the left-hand side of (17). The later can be done differently using one of the two “high-school level” techniques: adding and subtracting or multiplying and dividing. The first approach results in significantly shorter expressions for the right-hand sides involving  $\ddot{\theta}$  and the second one in much longer ones but independent on  $\ddot{\theta}$ . In particular, one can obtain a system in the following form

$$\begin{aligned} \ddot{y}_1 &= v_1, \\ \ddot{y}_2 &= v_2, \\ W &= \alpha(\theta)\ddot{\theta} + \beta(\theta)\dot{\theta}^2 + \gamma(\theta) = g_{y1}(\theta, \dot{\theta}, \ddot{\theta}, y_1, \dot{y}_1) y_1 \\ &\quad + g_{y2}(\theta, \dot{\theta}, \ddot{\theta}, y_2, \dot{y}_2) y_2 + g_{dy1}(\theta, \dot{\theta}, y_1, \dot{y}_1) \dot{y}_1 \\ &\quad + g_{dy2}(\theta, \dot{\theta}, y_2, \dot{y}_2) \dot{y}_2 + g_{v1}(\theta, y_1) v_1 + g_{v2}(\theta, y_2) v_2 \end{aligned} \quad (25)$$

It is left to notice, that since

$$f_1(\theta_*(t), \dot{\theta}_*(t), 0, 0, 0, 0) \equiv f_2(\theta_*(t), \dot{\theta}_*(t), 0, 0, 0, 0) \equiv 0,$$

one can rewrite these functions as

$$\begin{aligned} f_1(\theta, \dot{\theta}, y_1, y_2, \dot{y}_1, \dot{y}_2) &= f_{1y1}(t) y_1 + f_{1y2}(t) y_2 \\ &\quad + f_{1dy1}(t) \dot{y}_1 + f_{1dy2}(t) \dot{y}_2 + f_{1I}(t) I + \dots, \\ f_2(\theta, \dot{\theta}, y_1, y_2, \dot{y}_1, \dot{y}_2) &= f_{2y1}(t) y_1 + f_{2y2}(t) y_2 \\ &\quad + f_{2dy1}(t) \dot{y}_1 + f_{2dy2}(t) \dot{y}_2 + f_{2I}(t) I + \dots, \end{aligned} \quad (26)$$

where by “...” we denote higher-order terms in the linearization variables  $y, \dot{y}$ , and  $I$ .

Finally, since [13]

$$\frac{d}{dt} I(\theta(t), \dot{\theta}(t)) = \dot{\theta} \left\{ \frac{2}{\alpha(\theta)} W - \frac{2\beta(\theta)}{\alpha(\theta)} I \right\},$$

one obtains a linearization of the continuous part of the transverse dynamics, described by the linear system

$$\dot{\zeta} = \left( A(t) + B(t)K(t) \right) \zeta, \quad (27)$$

where  $\zeta$  gives linear parts of the deviations from zeros for the components of  $x_{\perp} = [I, y_1, y_2, \dot{y}_1, \dot{y}_2]^T$ ,

$$A(t) = \begin{bmatrix} a_{11}(t) & a_{12}(t) & a_{13}(t) & a_{14}(t) & a_{15}(t) \\ 0 & 0 & 0 & 1 & 0 \\ 0 & 0 & 0 & 0 & 1 \\ 0 & 0 & 0 & 0 & 0 \\ 0 & 0 & 0 & 0 & 0 \end{bmatrix}, \quad (28)$$

$$B(t) = \begin{bmatrix} b_1(t) & 0 & 0 & 1 & 0 \\ b_2(t) & 0 & 0 & 0 & 1 \end{bmatrix}^T,$$

$$K(t) = \begin{bmatrix} f_{1I}(t) & f_{1y1}(t) & f_{1y2}(t) & f_{1dy1}(t) & f_{1dy2}(t) \\ f_{2I}(t) & f_{2y1}(t) & f_{2y2}(t) & f_{2dy1}(t) & f_{2dy2}(t) \end{bmatrix},$$

$$\begin{aligned} a_{11}(t) &= -m_*(t)\beta(\theta_*(t)), & m_*(t) &= 2\dot{\theta}_*(t)/\alpha(\theta_*(t)), \\ b_1(t) &= m_*(t)g_{v1}(\theta_*(t), 0), & b_2(t) &= m_*(t)g_{v2}(\theta_*(t), 0), \\ a_{12}(t) &= m_*(t)g_{y1}(\theta_*(t), \dot{\theta}_*(t), \ddot{\theta}_*(t), 0, 0), \\ a_{13}(t) &= m_*(t)g_{y2}(\theta_*(t), \dot{\theta}_*(t), \ddot{\theta}_*(t), 0, 0), \\ a_{14}(t) &= m_*(t)g_{dy1}(\theta_*(t), \dot{\theta}_*(t), 0, 0), \\ a_{15}(t) &= m_*(t)g_{dy2}(\theta_*(t), \dot{\theta}_*(t), 0, 0). \end{aligned}$$

It is left to compute:

- (1) approximations for  $\phi_1(\theta)$  and  $\phi_2(\theta)$  and their two derivatives with the help of (16), based on the desired solution of the closed-loop system (14),
- (2) the desired solution  $\theta_*(t)$  of (17) with its derivatives,
- (3) the precise expressions or approximations for the coefficients of the expansions (26).

The first two tasks are easy to accomplish. Computing the first four coefficients in each of the two expansions (26) can be done evaluating the appropriate partial derivatives. The last term can be computed using the formulae

$$\begin{aligned} f_{1I,2I}(t) &= \left[ \dot{\theta}_*(t) \frac{\partial f_{1,2}(\cdot)}{\partial \dot{\theta}} - \ddot{\theta}_*(t) \frac{\partial f_{1,2}(\cdot)}{\partial \theta} \right] \Big|_{\substack{\theta=\theta_*(t), \dot{\theta}=\dot{\theta}_*(t) \\ y=0, \dot{y}=0}} \\ &\quad / \left[ 2 \left( \dot{\theta}_*(t) \right)^2 + 2 \left( \ddot{\theta}_*(t) \right)^2 \right]. \end{aligned}$$

The computed transverse linearization (27) should run for a fixed period of time of duration  $T_h$ . After that, a jump in the values of  $\zeta$  should occur and be followed by continuous dynamics similar to (27) and another jump. We now are in position to define jumps due to instantaneous impacts and switching of the supporting legs.

#### 1.4 Transverse Linearization for the Closed-Loop System

The linearization of the updating law map (3) with (4) is computed evaluating the corresponding Jacobian at  $x_T$

$$\delta x_{t+} = (dF) \delta x_{T_h-} \quad (29)$$

Now, we define the projections needed for modified linearization of the updating law. The values of components of  $\zeta(T_h-) \in \mathbb{R}^5$  should first be related to the corresponding values of components of  $x(T_h-) \in \mathbb{R}^6$ . Hence, we need to obtain the linearization of the relations

$$y_1 = q_2 - \phi_1(q_1), \quad y_2 = q_3 - \phi_2(q_1),$$

$$\dot{y}_1 = \dot{q}_2 - \phi_1'(q_1)\dot{q}_1, \quad \dot{y}_2 = \dot{q}_3 - \phi_2'(q_1)\dot{q}_1,$$

and  $I = I(q_1, \dot{q}_1)$ , defined by (21), in a vicinity of the desired trajectory at  $t = T_h$ . At an arbitrary moment of

time we have the next relation between the linear parts of the increments of the transversed coordinates in  $\mathbb{R}^5$  and the linear parts of the generalized coordinates in  $\mathbb{R}^6$ :

$$[\Delta I \ \Delta y^T \ \Delta \dot{y}^T]^T = L(t) [\Delta q^T \ \Delta \dot{q}^T]^T,$$

where using the easy to check formulae

$$\left. \frac{\partial I}{\partial \theta} \right|_{\substack{\theta=\theta_*(t) \\ \dot{\theta}=\dot{\theta}_*(t)}} = -2\ddot{\theta}_*(t), \quad \left. \frac{\partial I}{\partial \dot{\theta}} \right|_{\substack{\theta=\theta_*(t) \\ \dot{\theta}=\dot{\theta}_*(t)}} = 2\dot{\theta}_*(t), \quad (30)$$

one obtains

$$L(t) = \begin{bmatrix} -2\ddot{\theta}_*(t) & 0 & 0 & 2\dot{\theta}_*(t) & 0 & 0 \\ -\phi'_1(\theta_*(t)) & 1 & 0 & 0 & 0 & 0 \\ -\phi'_2(\theta_*(t)) & 0 & 1 & 0 & 0 & 0 \\ -\phi''_1(\theta_*(t))\dot{\theta}_*(t) & 0 & 0 & -\phi'_1(\theta_*(t)) & 1 & 0 \\ -\phi''_2(\theta_*(t))\dot{\theta}_*(t) & 0 & 0 & -\phi'_2(\theta_*(t)) & 0 & 1 \end{bmatrix}. \quad (31)$$

To derive an inverse transformation, we notice that<sup>2</sup>

$$n(t) = [\dot{q}_*^T(t) \ \ddot{q}_*^T(t)]^T \quad (32)$$

is orthogonal to  $S(t)$ , the moving Poincaré section at time  $t$ ; so that  $\zeta(t) \in TS(t)$ , the tangent to  $S(t)$ . Therefore,

$$\zeta = [\Delta I \ \Delta y^T \ \Delta \dot{y}^T]^T \in TS(t) \cong \mathbb{R}^5 \implies$$

$$\mathbb{R}^6 \supset TS(t) \ni \Delta x = \begin{bmatrix} \Delta q \\ \Delta \dot{q} \end{bmatrix} = \begin{bmatrix} L(t) \\ n^T(t) \end{bmatrix}^{-1} \begin{bmatrix} \zeta \\ 0 \end{bmatrix}. \quad (33)$$

It is important to realize at this point that the tangent plane to  $\Gamma_+$ , which is equal to

$$T\Gamma_+ = \{\delta x_{T_h-} \in \mathbb{R}^6 : m_1^T \delta x_{T_h-} = 0\},$$

where  $m_1^T = [0, 1, 0, 0, 0, 0]$ , computed from (6), is different from

$$TS(T_h) = \{\Delta x_{T_h-} \in \mathbb{R}^6 : n^T(T_h) \Delta x_{T_h-} = 0\},$$

where  $n(T_h)$  is given by (32). Therefore, the needed projection of  $TS(T_h)$  onto  $T\Gamma_+$  is not trivial. This transformation can be obtained taking

$$\delta x_{T_h-} = \Delta x_{T_h-} + f(x_*(T_h), u_*(T_h)) \tau_-, \quad (34)$$

where  $f(x_*(T_h), u_*(T_h)) = n(T_h)$  according to footnote 2,

$$\tau_- = -\frac{\Delta q_2(T_h-)}{\phi'_1(\theta_*(T_h))\dot{\theta}_*(T_h)} \iff m_1^T \delta x_{T_h-} = 0. \quad (35)$$

Using the coordinate transformation (33) we have

$$\Delta x_{T_h-} = \begin{bmatrix} L(T_h) \\ n^T(T_h) \end{bmatrix}^{-1} \begin{bmatrix} \zeta(T_h-) \\ 0 \end{bmatrix}. \quad (36)$$

Summarizing, the combination of (34), (35), and (36) defines the projection operator

$$\delta x_{T_h-} = P_{n(T_h)}^- \zeta(T_h-),$$

$$P_{n(T_h)}^- = \left( I_6 - \frac{n(T_h) m_1^T}{n^T(T_h) m_1} \right) \begin{bmatrix} L(T_h) \\ n^T(T_h) \end{bmatrix}^{-1} \begin{bmatrix} I_5 \\ 0_{1 \times 5} \end{bmatrix}. \quad (37)$$

For the other projection, one similarly obtains

$$\zeta(T_h+) = P_{n(0)}^+ \delta x_{T_h+},$$

$$P_{n(0)}^+ = L(0) P \left( I_6 - \frac{n(0) n^T(0)}{n^T(0) n(0)} \right). \quad (38)$$

Finally, the transverse linearization for the system (5) is a  $2T_h$ -periodic linear hybrid system defined over each period of time  $t \in [0, 2T_h]$  as follows

<sup>2</sup> This vector is a solution of  $L(t)n(t) = 0$ . Note that  $n(t) = f(x_*(t), u_*(t))$  where  $u_*(t)$  is the open-loop control signal consistent with the desired motion.

$$\begin{aligned} \dot{\zeta} &= \left( A_1(t) + B_1(t) K_1(t) \right) \zeta, & \text{for } 0 < t < T_h, \\ \zeta(T_h+) &= (d^{TS} F^{(1)}) \zeta(T_h-), \\ \dot{\zeta} &= \left( A_2(t) + B_2(t) K_2(t) \right) \zeta, & \text{for } T_h < t < 2T_h, \\ \zeta(2T_h+) &= (d^{TS} F^{(2)}) \zeta(2T_h-), \end{aligned} \quad (39)$$

where  $A_1(t) = A_2(t) = A(t)$  and  $B_1(t) K_1(t) = B_2(t) K_2(t) = B(t) K(t)$  are defined by (28), and  $(d^{TS} F^{(2)}) = (d^{TS} F^{(1)}) = P_{n(0)}^+ (dF) P_{n(T_h)}^-$  are defined by (38), (29), and (37). Here, the similarity of the two different phases of the motion (continuous plus discrete) is due to symmetry of the legs and identical controllers.

### 1.5 Stability Analysis Using the Transverse Linearization

The solution of the transverse linearization dynamics (39) at the end of the cycle, i.e. at  $t = 2T_h$ , initiated at  $\zeta(0)$  is given by the following formula

$$\zeta(2T_h) = \Psi \zeta(0),$$

$$\text{where } \Psi = \left( P_{n(0)}^+ (dF) P_{n(T_h)}^- \Phi(T_h) \right)^2, \quad (40)$$

$$\dot{\Phi}(t) = (A(t) + B(t) K(t)) \Phi(t), \quad \Phi(0) = I_5. \quad (41)$$

The eigenvalues of the matrix  $\Psi$

$$0.36377, \quad -0.01248 \pm 0.00492i, \quad -0.00948, \quad 0.00278$$

are inside the unit circle in the complex plane. Hence, the system (39) is exponentially stable and the desired trajectory of the nonlinear closed-loop system (5), (9), (12) is (locally) orbitally exponentially stable. The maximal absolute value of the eigenvalues is approximately equal to 0.36377. This number is an estimate of the stability degree in a vicinity of the desired trajectory, i.e. the rate of reduction of the distance from the desired orbit.

It is of interest to notice that the maximal absolute values of the eigenvalues of the matrix  $\Phi(T_h)$ , which corresponds to the continuous dynamics, is greater than 1.5996 and, therefore, the stability is insured only by the impact, i.e. essentially by a good choice of the imposed constraint.

The eigenvalues of the transition matrix  $\Psi$ , given by (40), are equal to the eigenvalues of the 5-dimensional Poincaré map for the impulsive system [11], see also [7].

### 1.6 Redesigning a stabilizing feedback controller

One of the consequences of the transverse-linearization-based analysis given in the previous section is that taking

$$v = K(\tau) [I(q_1, \dot{q}_1), y_1, y_2, \dot{y}_1, \dot{y}_2]^T \quad (42)$$

in combination with the feedback transformation, similar to (9) but written for the outputs (22),

$$u = \left( J(q_1, \dot{q}_1) \begin{bmatrix} 0_{3 \times 2} \\ M^{-1}(q) B \end{bmatrix} \right)^{-1} \left( v - J(q_1, \dot{q}_1) \begin{bmatrix} \dot{q} \\ M^{-1}(q) (-C(q, \dot{q}) \dot{q} - G(q)) \end{bmatrix} \right), \quad (43)$$

and with a time-stamp of the projection onto the desired trajectory  $\tau = \mathcal{T}(\theta, \dot{\theta}) \in [0, T_h)$ , which in our case can be taken as  $\mathcal{T}(\theta, \dot{\theta}) = T_h (\theta - \theta_*(0_+)) / (\theta_*(T_h-) - \theta_*(0_+)) \bmod T_h$ , during the first half of the period, and a similarly

defined controller for the second part, one obtains an orbitally exponentially stabilizing controller, provided

$$\mathcal{J}\{K(t)\} = \max_{1 \leq i \leq n} \left\{ \left| \text{eig}_i \{ P_{n(0)}^+ (dF) P_{n(T_h)}^- \Phi(T_h) \} \right| \right\} < 1, \quad (44)$$

where  $\Phi(T_h)$  is computed solving (41) and  $\text{eig}_i\{\cdot\}$  denotes the  $i$ th eigenvalue.

It is tempting to simplify the feedback controller by choosing (42) with a constant matrix  $K$ . The coefficients of this matrix can be obtained using a simple minimization procedure for (44). The result of such a search is

$$\bar{K} = \begin{bmatrix} -0.0063 & -17.9205 & 0.1516 & -6.3287 & -0.6052 \\ -1.9941 & -0.0836 & -6.7921 & -0.4683 & -5.1153 \end{bmatrix}$$

with  $\mathcal{J}(\bar{K}) = 0.138$  being the value of (44).

The results of numerical simulations with all three feedback controllers described here are omitted due to space limitations. We have observed that the feedback controller based on the constant gain  $\bar{K}$  has the best local convergence rate but the smallest region of attraction.

## 2. CONCLUSION

In the situation, when the goal of control design is orbital exponential stabilization, computing a linearization around the desired trajectory is not trivial. Such a linearization should be computed after the one-dimensional dynamics along the trajectory is separated. Although no analytical technique is known for general nonlinear systems, it can be done for systems, dynamics of which can be described by controlled Euler-Lagrange equations. It has been recently shown how to use the transverse linearization technique for control design and stability analysis for smooth systems with underactuation degree one.

Bipedal robots can often be described by models in this class during the swing phase of motion, after which an impact with environment occurs. Such an impact can be modeled as an impulse effect, which complements the continuous-time part of the dynamics. In this paper, we have suggested a procedure of modifying the transverse linearization in order to incorporate impulse effects. The resulting dynamics consist of a linear system and a linear updating law, acting at fixed time instances.

Derivations are shown for a particular model of a three-link walking robot. We have computed a transverse linearization and have shown how to use it for analysis of a known feedback controller and for designing alternative ones.

## 3. ACKNOWLEDGMENTS

For numerical simulations, we have partially used the Matlab code provided by the authors of [18], see: [http://www.mecheng.osu.edu/~westerve/biped\\_book/](http://www.mecheng.osu.edu/~westerve/biped_book/).

## REFERENCES

- [1] Bainov D.D. and P.S. Simeonov, *Systems with Impulse Effects: Stability, Theory and Applications*, Ellis Horwood, Chichester, UK, 1989.
- [2] Bhat S.P. and D.S. Bernstein, "Continuous finite-time stabilization of the translational and rotational double integrators," *IEEE Trans. Autom. Control*, **43**(5): 678–682, 1998.
- [3] Brogliato B., *Nonsmooth Impact Dynamics: Models, Dynamics, and Control*, London, U.K.: Springer-Verlag, 1996.
- [4] Chevallereau C., G. Abba, Y. Aoustin, F. Plestan, E.R. Westervelt, C. Canudas-de-Wit, and J.W. Grizzle, "Rabbit: A testbed for advanced control theory," *IEEE Control Systems Magazine*, **23**(5): 57–79, 2003.
- [5] Grizzle J.W., G. Abba, and F. Plestan, "Proving asymptotic stability of a walking cycle for a five DOF biped robot model," Proc. *2nd Intern. Conf. Clim. and Walking Robots*, Portsmouth, UK, 1999.
- [6] Grizzle J.W., G. Abba, and F. Plestan, "Asymptotically stable walking for biped robots: Analysis via systems with impulse effects," *IEEE Trans. Autom. Control*, **46**(1): 51–64, 2001.
- [7] Hiskins I.A., "Stability of hybrid system limit cycles: application to the compass gait biped robot," Proc. *40th Conf. Decision & Contr.*, Orlando, USA, 2001.
- [8] Hurmuzlu Y. and D.B Marghitu, "Rigid body collisions of planar kinematic chains with multiple contact points," *Int. J. Robot. Research*, **13**(1): 82–92, 1994.
- [9] McGeer T., "Passive dynamic walking," *Int. J. Robot. Research*, **9**(2): 62–82, 1990.
- [10] Morris B. and J.W. Grizzle, "Hybrid invariant manifolds in systems with impulse effects with application to periodic locomotion in bipedal robots," to appear in *IEEE Trans. Autom. Control*.
- [11] Nersesov S., V. Chellaboina, and W. Haddad, "A generalization of Poincaré's theorem to hybrid and impulsive dynamical systems," *Int. J. Hybrid Systems*, **2**: 35–51, 2002.
- [12] Shiriaev A.S., L.B. Freidovich, and I.R. Manchester, "Can we make a robot ballerina perform a pirouette? Orbital stabilization of underactuated mechanical systems," Proc. *3rd IFAC Work. Periodic Control Systems*, St. Petersburg, Russia, 2007.
- [13] Shiriaev A.S., J.W. Perram, and C. Canudas-de-Wit, "Constructive tool for orbital stabilization of underactuated nonlinear systems: virtual constraints approach," *IEEE Trans. Autom. Control*, **50**(8): 1164–1176, 2005.
- [14] Shiriaev A.S., A. Robertsson, J.W. Perram, and A. Sandberg, "Periodic motion planning for virtually constrained mechanical system," *Systems & Control Letters*, **55**(11): 900–907, 2006.
- [15] Song, G. and M. Zefran, "Stabilization of hybrid periodic orbits with application to bipedal walking," Proc. *Amer. Contr. Conf.*, Minneapolis, USA, 2006.
- [16] Spong M.W. "Partial feedback linearization of underactuated mechanical systems," Proc. *Intern. Conf. Intell. Robots & Systems*, Munich, Germany, 2004.
- [17] Spong M.W., S. Hutchinson, and M. Vidyasagar, *Robot modeling and control*, John Wiley & Sons, 2006.
- [18] Westervelt E.R., J.W. Grizzle, C. Chevallereau, J.H. Choi, and B. Morris, *Feedback Control of Dynamic Bipedal Robot Locomotion*, Taylor & Francis / CRC Press, 2007.
- [19] Westervelt, E.R., J.W. Grizzle, and D.E. Koditschek, "Hybrid zero dynamics of planar biped walkers," *IEEE Trans. Autom. Control*, **48**(1): 42–56, 2003.
- [20] Ye H., A.N. Michel, and L. Hou, "Stability theory for hybrid dynamical systems," *IEEE Trans. Autom. Control*, **43**(4): 461–474, 1998.